Supporting Information

Ten polymorphs of $NH^+\cdots N$ hydrogen bonded DABCO complexes: Supramolecular origin of giant anisotropic dielectric response in polymorph V

*Anna Olejniczak and Andrzej Katrusiak**

Faculty of Chemistry, Adam Mickiewicz University, Grunwaldzka 6, 60-780 Poznań, Poland

Marek Szafrański

Faculty of Physics, Adam Mickiewicz University, Umultowska 85, 61-614 Poznań, Poland

*Corresponding author. E-mail: karan@amu.edu.pl

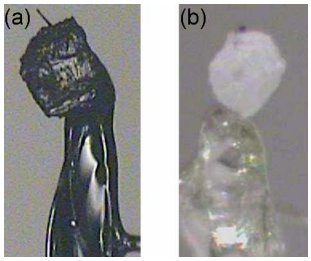

Figure S1. Crystal of dabcoHI recovered from the DAC chamber: (a) in phase VI at ambient conditions obtained from high-pressure phase VII shown in Fig. 1) and (b) in phase IV at atmospheric pressure and 400 K, obtained from high-pressure phase IX. The sample is glued with nail varnish to a glass fiber.

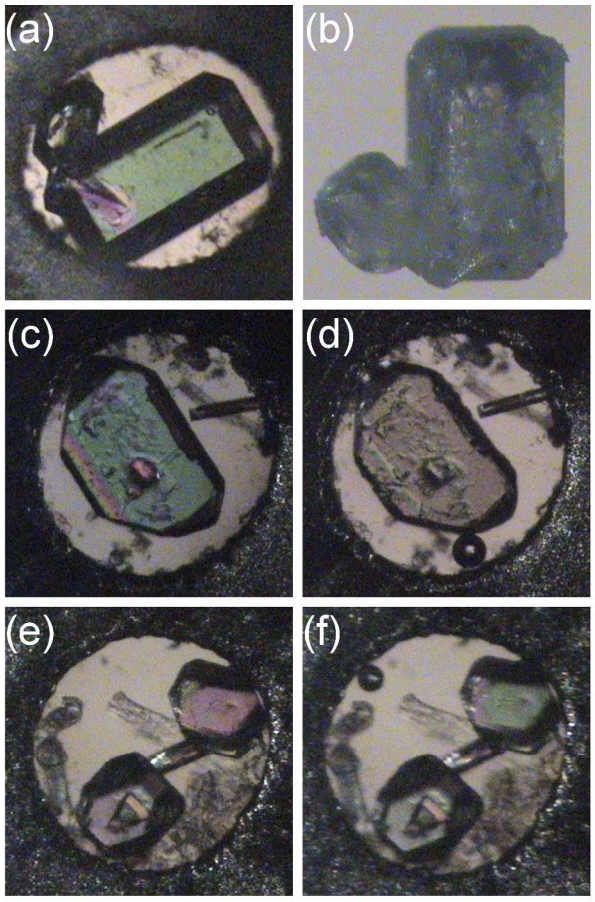

Figure S2. Stages of transformation of crystal in phase IX to phase VI: (a) single crystal in phase IX at 0.30 GPa; (b) the same crystal removed from the DAC; (c) another single crystal in phase IX at 0.40 GPa; (d) the same crystal in phase VI still in the DAC after releasing pressure (an air bubble is visible by the bottom edge of the gasket); (e) crystals in phase IX in another experiment; and (f) the same crystals immediately after releasing pressure (air bubble by the top-left edge). Photographs c-d and e-f were taken in polarized light for the same orientation of the DAC and the samples and the transformation causes color changes. A few seconds after transformation crackes develop in the sample (b).

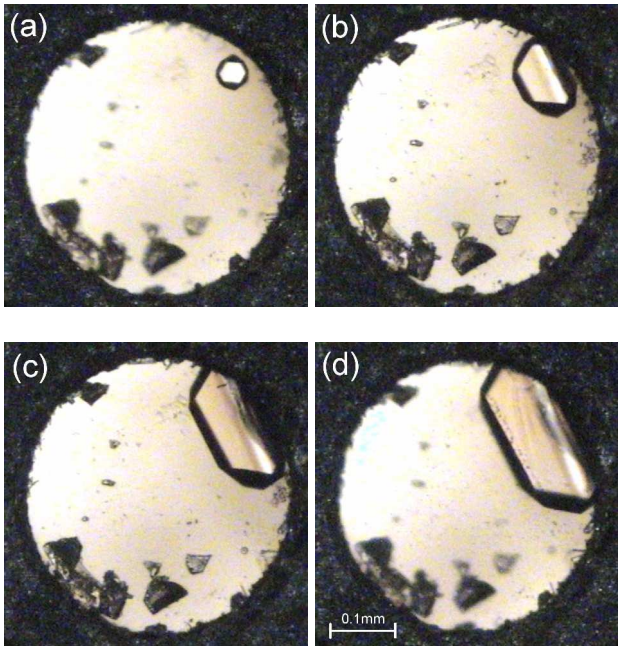

Figure S3. Stages of dabcoHI polymorph IX single crystal isochoric growth: (a) one grain at 413 K; (b) this grain at 393 K; (c) at 363 K; and (d) at 296 K/1.00(5) GPa.

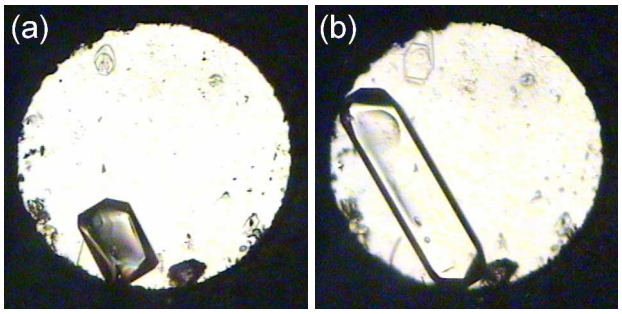

Figure S4. Isochoric growth of a single crystal of dabcoHI polymorph IX from aqueous solution: (a) at 353 K; and (b) at 296 K/0.50(5) GPa. The ruby chip for pressure calibration is visible at the bottom edge of the gasket.

Table S1. Crystal data and structure-refinements details for high-pressure measurements of dabcoHI.

Phase	VII	VIII	IX	IX
Pressure (GPa)	0.20(5)	0.20(5)	0.50(5)	1.00(5)
Temperature (K)	296(2)	296(2)	296(2)	296(2)
Formula weight	240.08	240.08	240.08	240.08
Wavelength (Å)	0.71073	0.71073	0.71073	0.71073
Crystal system	Orthorhombic	Orthorhombic	Monoclinic	Monoclinic
Space group	*Pbcm*	*Cmm*2	*P*2/*c*	*P*2/*c*
Unit cell dimensions (Å,°)				
a	5.3423(11)	10.638(2)	8.4180(17)	8.3430(17)
b	12.200(2)	13.125(3)	6.0961(12)	5.9730(12)
c	13.309(3)	6.1430(12)	16.690(3)	16.525(3)
β	90.00	90.00	102.04(3)	101.91(3)
Volume ($Å^3$)	867.4(3)	857.7(3)	837.6(3)	805.8(3)
Z	4	4	4	4
Calculated density (g/cm^3)	1.838	1.859	1.904	1.979
Absorption coefficient (mm^{-1})	3.618	3.659	3.747	3.895
F(000)	464	464	464	464
Crystal size (mm)	0.53/0.26/0.10	0.24/0.12/0.11	0.21/0.16/0.11	0.26/0.11/0.10
θ-range for data collection (°)	3.34 to 29.76	2.46 to 29.54	3.34 to 29.28	2.49 to 29.56
Min/max indices:h, k, l	-6/6,-16/17,-13/13	-10/10,-16/17,-7/7	-7/7,-8/8,-14/14	-11/10,-4/4,-21/20
Reflect. Collected/unique	6358/585	2875/667	5274/490	4812/755
R_{int}	0.0637	0.0984	0.0569	0.0819
Refinement method	Full-matrix least-squares on F^2			
Completeness (%)	45.3	50.3	21.3	33.3
Data/restrains/parameters	585/0/32	667/8/50	490/0/43	755/0/78
Goodness-of-fit on F^2	1.410	1.057	1.389	1.209
Final R_1/wR_2 ($I>2\sigma_1$)	0.1078/ 0.1380	0.0439/0.0880	0.0617/0.0868	0.0757/0.1403
R_1/wR_2 (all data)	0.1223/0.1422	0.0596/0.0949	0.0743/0.0900	0.0847/0.1471
Weighting parameters w_1,w_2 [a)]	0.0000,12.79	0.0437,1.15	0.0205,2.40	0.07.17,2.40
Largest diff. peak/hole ($e.Å^{-3}$)	0.445/-0.630	0.445/-0.557	0.237/-0.240	0.497/-0.477

[a] $w=1/(\sigma^2 F_o^2+w_1^2*P^2+w_2*P)$, where $P=(\mathrm{Max}(F_o^2,0)+2*F_c^2)/3$

Table S2. Crystal data and structure refinements details for low-temperature measurements of dabcoHI.

Phase	IV	VI	VI	VI	VI
Pressure (MPa)	0.10	0.10	0.10	0.10	0.10
Temperature (K)	400(2)	296(2)	220(2)	160(2)	100(2)
Formula weight	240.08	240.08	240.08	240.08	240.08
Wavelength (Å)	0.71073	0.71073	0.71073	0.71073	0.71073
Crystal system	Orthorhombic	Orthorhombic	Orthorhombic	Orthorhombic	Orthorhombic
Space group	*Pmm*2	$Pmc2_1$	$Pmc2_1$	$Pmc2_1$	$Pmc2_1$
Unit cell dimensions (Å,°)	6.622(8)	6.6567(10)	6.6529(13)	6.6518(13)	6.6598(12)
a	5.343(7)	5.3409(8)	5.3357(11)	5.3302(11)	5.3322(10)
b	6.228(12)	12.2343(15)	12.120(2)	12.065(2)	12.041(2)
c					
β					
Volume ($Å^3$)	220.3(6)	434.96(11)	430.23(15)	427.77(15)	427.59(13)
Z	1	2	2	2	2
Calculated density (g/cm^3)	1.809	1.833	1.853	1.864	1.865
Absorption coefficient (mm^{-1})	3.561	3.608	3.647	3.668	3.670
F(000)	116	232	232	232	232
Crystal size (mm)	0.15/0.10/0.10	0.18/0.15/0.10	0.18/0.15/0.10	0.18/0.15/0.10	0.18/0.15/0.10
θ-range for data collection (°)	3.27 to 28.34	3.06 to 27.87	3.06 to 27.87	3.06 to 27.89	3.06 to 29.29
Min/max indices:h, k, l	-8/8, -6/6, -4/7	-8/8, -6/6, -15/15	-8/8, -6/6, -12/12	-8/8, -6/6, -12/12	-7/8, -5/7, -15/15
Reflect. Collected/ unique	657/404	3435/947	1601/740	1577/729	2666/1104
R_{int}	0.2226	0.0777	0.0897	0.0853	0.0874
Refinement method	Full-matrix least-squares on F^2				
Completeness (%)	84.9	95.6	82.1	81.6	92.2
Data/restrains/parameters	404/1/26	947/1/49	740/1/49	729/1/44	1104/1/28
Goodness-of-fit on F^2	1.033	1.082	1.046	1.067	1.117

Final R_1/wR_2 ($I>2\sigma_1$)	0.0745/0.1725	0.0418/0.1189	0.0494/0.1290	0.0510/0.1324	0.0632/0.1735
R_1/wR_2 (all data)	0.1300/0.2072	0.0427/0.1204	0.0501/0.1302	0.0512/0.1327	0.0651/0.1758
Weighting parameters w_1,w_2 [a)]	0.0806,0.00	0.0910,0.00	0.0992,0.00	0.1050,0.00	0.1323,00.00
Largest diff. peak/hole (e.Å^{-3})	1.358/-0.936	0.775/-1.536	0.913/-1.303	1.349/-1.480	2.121/-1.852

[a)] $w=1/(\sigma^2F_o^2+w_1^2*P^2+w_2*P)$, where $P=(\mathrm{Max}(F_o^2,0)+2*F_c^2)/3$

Table S3. The shortest intermolecular interactions for high-pressure dabcoHI polymorphs.

	VII	VIII	IX	IX
p(GPa)	0.20(5)	0.20(5)	0.50(5)	1.00(5)
T(K)	296	296	296	296
N-H···N^{i}	1.91/2.82(2)/175.77	1.86/2.75(2)/164.90	1.87/2.78(2)/176.42	1.83/2.74(2)/177.69
N-H···N^{ii}		2.05/2.94(2)/165.29	1.98/2.86(1)/163.78	2.00/2.88(2)/162.85
C-H···I^{iii}	3.02/3.94(1)/159.48	3.03/3.99(1)/173.01	3.00/3.97(3)/176.35	2.94/3.91(1)/178.10
C-H···I^{iv}	3.09/4.03(1)/161.71	3.13/3.99(1)/148.94	3.01/3.96(3)/169.04	2.95/3.90(1)/165.75
C-H···I^{v}	3.26/4.01(2)/135.52	3.25/4.03(2)/139.51	3.08/3.95(3)/148.95	3.00/3.91(1)/147.45
C-H···I^{vi}			3.11/3.97(3)/148.26	3.08/3.92(1)/145.68
C-H···I^{vii}			3.13/3.96(3)/144.66	3.09/3.92(2)/144.43
C-H···I^{viii}			3.19/4.00(3)/142.24	3.09/3.93(2)/145.56
C-H···I^{ix}			3.26/4.06(3)/141.75	3.13/3.97(2)/146.14
C-H···I^{x}			3.26/4.09(3)/144.98	3.13/3.97(2)/145.66
C-H···I^{xi}				3.28/4.02(2)/134.40

symmetry codes for phase VII: (i)1+x,y,z; (iii)1+x,y,0.5-z; (iv)x,y,z; (v)1-x,1-y,1-z;

symmetry codes for phase VIII: (i)-x,1-y,z; (ii)1-x,1-y,z; (iii)-x,1-y,-1+z; (iv)0.5-x,0.5-y,-1+z; (v)0.5-x,0.5-y,z

symmetry codes for phase IX: (i)-x,1-y,-z; (ii)1-x,y,0.5-z; (iii)-x,1+y,0.5-z; (iv)x,1-y,-0.5+z; (v)x,1+y,z; (vi)1-x,1+y,0.5-z; (vii)x,y,z; (viii)1-x,y,0.5-z; (ix)x,1+y,z; (x)1-x,1+y,0.5-z; (xi)x,-y,-0.5+z

Table S4. The shortest intermolecular interactions for low- and high-temperature dabcoHI polymorphs.

	IV	VI	VI	VI	VI
p(MPa)	0.1	0.1	0.1	0.1	0.1
T(K)	400	296	220(2)	160(2)	100(2)
N-H···N[i]	1.96/2.87(4)/176.97	1.90/2.81(1)/176.98	1.91/282(1)/176.24	1.88/2.79(1)/175.76	1.87/2.78(2)/178.44
C-H···I[ii]	3.10/4.03(2)/162.10	3.01/3.94(1)/159.89	3.00/3.92(1)/159.65	3.00/3.92(1)/159.19	3.00/3.92(1)/158.37
C-H···I[iii]	3.29/4.09(4)/140.64	3.09/4.02(1)/160.79	3.08/4.00(1)/160.17	3.06/3.99(1)/160.08	3.06/3.98(1)/159.62
C-H···I[iv]		3.27/4.03(1)/136.34	3.27/4.02(3)/134.78	3.27/4.11(2)/146.21	3.24/4.01(1)/136.80

symmetry codes for phase IV: (i)1-x,2-y,z; (ii)x,y,1+z; (iii)x,y,z

symmetry codes for phases VI: (i)x,1+y,z; (ii)1+x,1+y,z; (iii)x,y,z; (iv)-x,1-y,0.5+z

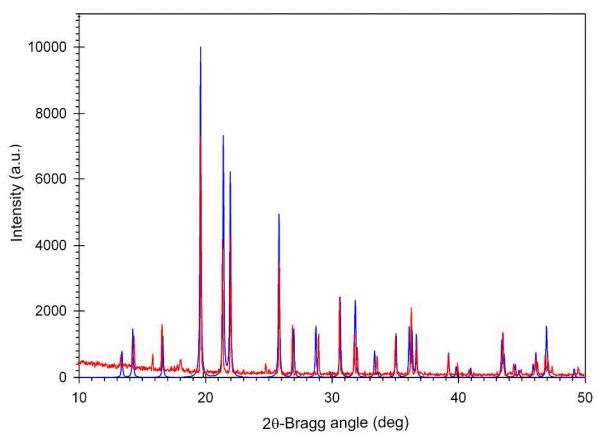

Figure S5. Powder pattern of dabcoHI structure in phase IV measured at 393 K (red) and generated (blue) from the single-crystal x-ray data. The reflection at 18° is an artifact, appearing in all the patterns, and arising from the scattering of x-rays on the elements of the oven used for heating the sample in the powder-diffraction experiments.

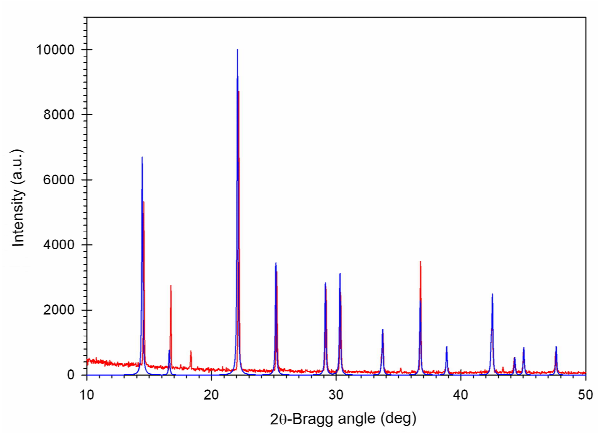

Figure S6. Powder pattern of dabcoHI structure in phase V measured at 333 K (red) and generated (blue) from the single-crystal x-ray data. The reflection at 18° is an artifact, appearing in all the patterns, and arising from the scattering of x-rays on the elements of the oven used for heating the sample in the powder-diffraction experiments.

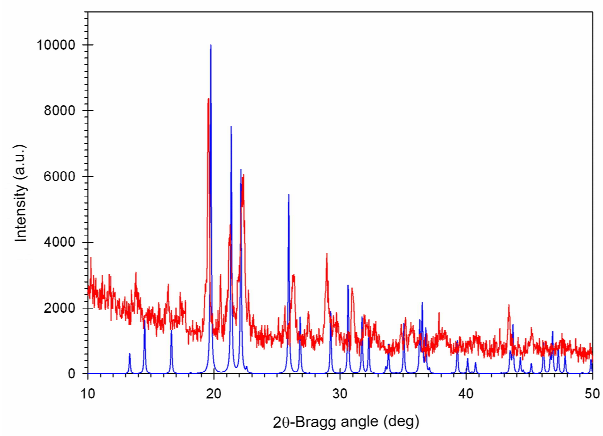

Figure S6. Powder pattern of dabcoHI structure in phase VI measured at 323 K (red) and generated (blue) from the single-crystal x-ray data at 296 K. The reflection at 18° is an artifact, appearing in all the patterns, and arising from the scattering of x-rays on the elements of the oven used for heating the sample in the powder-diffraction experiments.

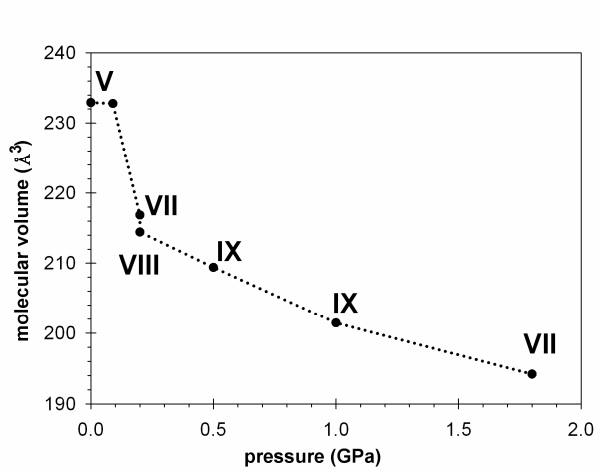

Figure S8. Molecular-volume in dabcoHI polymorphs measured by single-crystal x-ray diffraction at varied pressure. The Roman numbers label the dabcoHI polymorphs. The dotted line joining the points has been drawn for guiding the eye only.

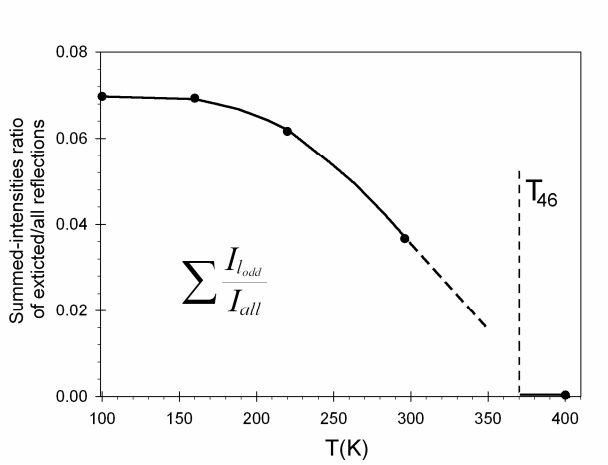

Figure S9. Temperature dependence of the $\sum I_{lodd} / \sum I_{all}$ for dabcoHI, illustrating the process of unit-cell parameter *c* doubling in phase VI below 370 K. According to the DSC measurements phase VI ($Pmc2_1$) is stable to 370 K and it transforms to phase IV at higher temperature ($c_{VI}=2\times c_{IV}$). T_{46} denotes the transition temperature between phases IV and VI (*cf.* Fig. 7a). The dashed part of the line indicates its possible values close to the transition temperature (the phase transition is first-order in character).

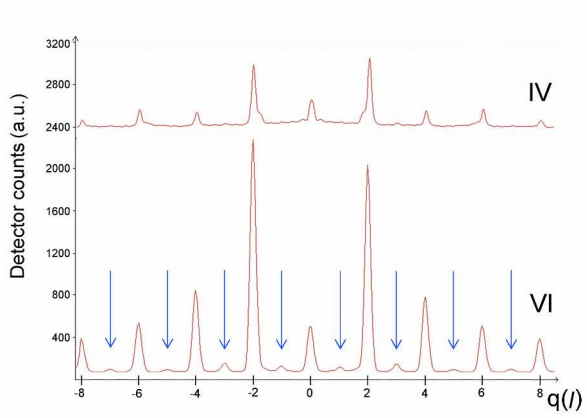

Figure S10. Profiles of detector counts along reciprocal lattice direction [02*l*], illustrating the intensities of reflections becoming extinct (indicated by arrows) on transformation of phase VI to IV [l_{odd} in the (02*l*) layer of phase VI].

Table S5. Modulation vectors **m** of $NH^+\cdots N$ bonded chains in dabcoHI polymorphs IV-IX, their modulation period (|**m**|), modulation amplitude (A), inclination of cations to the chain direction (α) and number of cations per one modulation period (n).

Polymorph	Chain direction	n	α (°)	|**m**| (Å)	A (Å)
IV	[010]	1	0	5.343	0
V	[001]	1	0	5.346	0
VI	[010]	1	1.7(3)	5.3409	0.040
VII	[100]	1	2.9(9)	5.3423	0.068
VIII	[100]	2	9.9(3)	10.638	0.464
IX	[201]	4	11.2(2)	22.398	1.109
IX	[201]	4	12.2(6)	22.239	1.202